AD-A138 725 THE UNSTEADY BOUNDARY LAYER ON AN ELLIPTIC CYLINDER FOLLOWING THE IMPULSI..(U) COLORADO UNIV AT BOULDER DEPT OF AEROSPACE ENGINEERING SCIENC.. 1/1

UNCLASSIFIED D F BILLINGS ET AL. 13 JAN 83 F/G 20/4 NL

END
DATE FILMED
4-84
DTIC

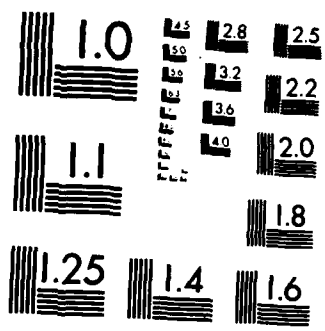

UNCLASSIFIED
SECURITY CLASSIFICATION OF THIS PAGE (When Data Entered)

(2)

REPORT DOCUMENTATION PAGE		READ INSTRUCTIONS BEFORE COMPLETING FORM
1. REPORT NUMBER AFOSR-TR- 84-0043	2. GOVT ACCESSION NO. AD-A138725	3. RECIPIENT'S CATALOG NUMBER
4. TITLE (and Subtitle) THE UNSTEADY BOUNDARY LAYER ON AN ELLIPTIC CYLINDER FOLLOWING THE IMPULSIVE ONSET OF TRANSLATIONAL AND ROTATIONAL MOTION		5. TYPE OF REPORT & PERIOD COVERED INTERIM 6. PERFORMING ORG. REPORT NUMBER
7. AUTHOR(s) D.F.Billings and C.-Y.CHOW		8. CONTRACT OR GRANT NUMBER(s) AFOSR-81-0037
9. PERFORMING ORGANIZATION NAME AND ADDRESS University of Colorado Boulder, CO 80309		10. PROGRAM ELEMENT, PROJECT, TASK AREA & WORK UNIT NUMBERS 61102F 2307/A2
11. CONTROLLING OFFICE NAME AND ADDRESS AFOSR/NA Bolling AFB, DC 20332		12. REPORT DATE JAN 10-13, 1983 13. NUMBER OF PAGES 8
14. MONITORING AGENCY NAME & ADDRESS(if different from Controlling Office)		15. SECURITY CLASS. (of this report) UNCLASSIFIED 15a. DECLASSIFICATION/DOWNGRADING SCHEDULE

16. DISTRIBUTION STATEMENT (of this Report)

Approved for public release; distribution unlimited.

17. DISTRIBUTION STATEMENT (of the abstract entered in Block 20, if different from Report)

18. SUPPLEMENTARY NOTES

Presented at the AIAA 21st Aerospace Sciences Meeting, Jan 10-13, 1983, Reno, Nevada

19. KEY WORDS (Continue on reverse side if necessary and identify by block number)

20. ABSTRACT (Continue on reverse side if necessary and identify by block number)

The fluid motion about an elliptic cylinder impulsively set into translational and rotational motion is obtained by the method of matched asymptotic expansions for small time and large Reynolds number. The constraint of the perturbation model is that the boundary layer thickness and the distance of travel are of the same asymptotic order. It is found that pitch-up motion or rotation accompanying translation at an angel of attack is indeed capable of preventing the early

BACK

DD FORM 1 JAN 73 1473 EDITION OF 1 NOV 68 IS OBSOLETE

unclassified
SECURITY CLASSIFICATION OF THIS PAGE (When Data Entered)

Cont'd #20 Abstract:

formation of a leading edge separation bubble. Even before evident in the streamline pattern, the incipient separation bubble is accompanied by a characteristic vorticity signature in the vicinity of the leading edge that is quite different from that with rotation. Further, the onset of an adverse pressure gradient is displaced rearward from its location for pure translation. The pre-Kutta condition lift evidently arises with the local acceleration that is a consequence of the displacement effect of the growing boundary layer.

AIAA-83

AIAA-83-0128
The Unsteady Boundary Layer on an Elliptic Cylinder Following the Impulsive Onset of Translational and Rotational Motion

D.F. Billings and C.-Y. Chow, Univ. of Colorado, Boulder, CO

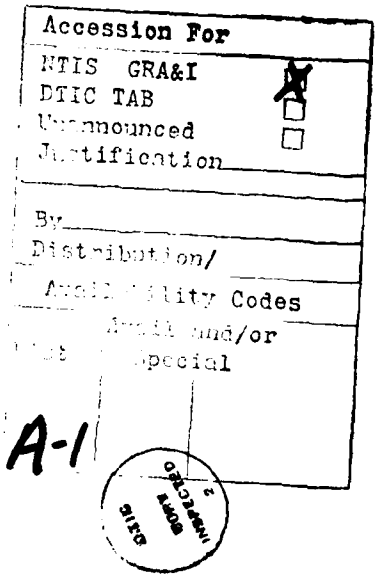

AIAA 21st Aerospace Sciences Meeting

January 10-13, 1983/Reno, Nevada

THE UNSTEADY BOUNDARY LAYER ON AN ELLIPTIC CYLINDER FOLLOWING THE IMPULSIVE ONSET OF TRANSLATIONAL AND ROTATIONAL MOTION

Dana Billings

and

Chuen-Yen Chow*
University of Colorado
Boulder, Colorado 80309

Abstract

The fluid motion about an elliptic cylinder impulsively set into translational and rotational motion is obtained by the method of matched asymptotic expansions for small time and large Reynolds number. The constraint of the perturbation model is that the boundary layer thickness and the distance of travel are of the same asymptotic order. It is found that pitch-up motion or rotation accompanying translation at an angle of attack is indeed capable of preventing the early formation of a leading edge separation bubble. Even before evident in the streamline pattern, the incipient separation bubble is accompanied by a characteristic vorticity signature in the vicinity of the leading edge that is quite different from that with rotation. Further, the onset of an adverse pressure gradient is displaced rearward from its location for pure translation. The pre-Kutta condition lift evidently arises with the local acceleration that is a consequence of the displacement effect of the growing boundary layer.

I. Introduction

The dynamic suppression or retardation of separation from an airfoil undergoing rapid pitching motion enables the airfoil to acheive an angle of attack that may be much larger than the steady flow stall incidence angle and yet retain an *intact* boundary layer. This is concomitant to the phenomena of dynamic stall. During this motion, and for unsteady motion in general, the presence of reversed flow adjacent to the body need not have any particular significance; it does not signal immediate separation in the Prandtl sense of gross departure of flow from the surface with the consequent complete alteration of the flow field.[1] Yet its presence seems to be implicated in the eventual breakdown of boundary layer flow, whether it occurs via the bursting of a leading edge separation bubble, perhaps fed by a thin layer of reverse flow that has advanced upstream along the surface to the neighborhood of the separation bubble, or by the thickening of this layer itself.[2] It was for insight into the delay of the onset of flow reversal and its spread that the present work was undertaken.

The approach taken is one that is recurrent in the literature; namely, the development of an asymptotic solution for boundary layer growth on a circular or elliptic cylinder in a short time interval following the impulsive onset of motion. The procedure is to iterate upon a basic solution, in this case, the Rayleigh solution for the (locally) flat, impulsively started plate. By continuing in this manner, Goldstein and Rosenhead[3] were able to extend Blasius's 1908 work to a third approximation, obtaining a coordinate-type expansion in small time for the boundary layer growth on a circular cylinder (see also Batchelor[4], Stuart[5]). Mutual interaction, however, between the growing boundary layer and the outer flow was excluded; the pressure distribution impressed upon the boundary layer, for instance, remained that of the unperturbed outer flow. Wang[6], therefore applied the technique of matched inner and outer expansions to his problem of the impulsively started elliptic cylinder. Like Goldstein and Rosenhead, he was able to trace the temporal appearance and spatial progression of reverse flow by solving for the time at which wall shear vanishes (if it does) at any surface location. His results, for the cylinder moving at an angle of attack, show reversed flow advancing upstream from the vicinity of the rear stagnation point and eventually merging with a slower-to-form reverse flow region near the leading edge (a separation bubble). For the present work, we adopt the method of Wang, with the addition of an impulsive onset of rotation.

II. Perturbation Model

Initially the fluid motion is everywhere irrotational except on the surface of the cylinder where viscous interaction requires that the fluid in contact with the surface by at rest relative to it and where, therefore, a surface of slip or vortex sheet exists. For a short time thereafter, the diffusion of vorticity is the dominant effect in the fluid close to the surface. It is this short time interval in the growth of the boundary layer that is the concern of the present study.

Posed in this way, it is perhaps natural to consider the problem as a singular coordinate-type perturbation problem for small values of the independent variable time and to apply matching in the coordinate normal to the surface to overcome the disparity in the inner and outer characterizations. Although there is nothing wrong with such an approach, we have instead chosen to formulate the problem as a parameter perturbation in a parameter ϵ which tends to zero as time tends to zero. It represents, in the domain of small time, a rescaling of the geometric time scale L/U_∞ (characteristic length and speed) analogous to the $R^{-\frac{1}{2}}$ (for Reynolds number R) rescaling of the coordinate normal to the surface which yields the familiar boundary layer equations.

For large R, another source of nonuniformity, and a practical concern in evaluating a series consisting of only a few terms, is the presence of ratios of the temporal perturbation quantity to R. With the introduction of ϵ, this nonuniformity can be expressed as $\epsilon^n \neq o(\epsilon/R)$ uniformly in R as $R \to \infty$. It becomes convenient, therfore, to establish a connection between the limit processes of $R \to \infty$ and $\epsilon \to 0$.

*Professor, Department of Aerospace Engineering Sciences. Member AIAA.

The simplest connection between the limit processes on R and ε is expressed by $R^{-1} \propto \varepsilon^k$ for $k \geq 0$. For a specific value of k, this is equivalent to an asymptotic order relation between the distance d that the body travels in time t at a speed U_c and the quantity $\delta = (\nu t)^{\frac{1}{2}}$ (ν is the kinematic viscosity) which characterizes the boundary layer thickness for unsteady fluid motion about a body starting from rest at t = 0. This follows from letting $d/L = U_c t/L = O(\varepsilon)$ and writing $\varepsilon^2/L^2 = R^{-1}d/L$. For large k, the boundary layer assumptions hold to a good approximation, that is, to a high order in ε. For smaller k, we may expect an earlier departure from strict boundary layer flow. Let us take the model relation $R^{-1} \propto \varepsilon$. The proportionality constant is then the local Reynolds number based on the length d and the boundary layer thickness is of the same asymptotic order as the distance of travel.

III. Formulation

Let us normalize the equations of motion with respect to the length L taken as half the distance between the focii of the elliptic body, the density of the incompressible fluid, and the characteristic velocity combination $U_c = U_s + \Omega L$ of the speed of the distant flow U_s, incident at an angle of attack α_0, and the rotational velocity ΩL (fig. 1). For convenience we shall define $L/U_c = \gamma$ so that $U_s/U_c = 1 - \gamma$. If in addition, we let T be the characteristic time, representing the small time scale of observation, the dimensionless parameters $U_c T/L$ and R are found to completely characterize the fluid motion for a given geometry of initial and boundary conditions. In accordance with the previous discussion, we take

$$\varepsilon = U_c T/L = \beta^{-2} R^{-1} \tag{1}$$

where β is a constant of order unity. Then the equations of motion for incompressible, two dimensional flow in a body fixed frame and elliptic cylindrical coordinates (ξ,η,z) become

$$\frac{\partial u}{\partial t} + \varepsilon\left[\frac{u}{h}\frac{\partial u}{\partial \xi} + \frac{v}{h}\frac{\partial u}{\partial \eta} + \frac{uv}{h^2}\frac{\partial h}{\partial \eta} - \frac{v^2}{h}\frac{\partial h}{\partial \xi}\right] = -\beta^2\varepsilon^2\left[\frac{1}{h}\frac{\partial}{\partial \xi}\left(\frac{1}{h^2}\frac{\partial hv}{\partial \eta}\right) - \frac{1}{h}\frac{\partial}{\partial \eta}\left(\frac{1}{h^2}\frac{\partial hu}{\partial \xi}\right)\right] - \varepsilon\frac{1}{h}\frac{\partial p}{\partial \eta} + 2\gamma\varepsilon v - \gamma^2\varepsilon\frac{\partial h}{\partial \xi} \tag{2}$$

$$\frac{\partial v}{\partial t} + \varepsilon\left[\frac{v}{h}\frac{\partial v}{\partial \xi} + \frac{u}{h}\frac{\partial v}{\partial \eta} + \frac{uv}{h^2}\frac{\partial h}{\partial \eta} - \frac{u^2}{h^2}\frac{\partial h}{\partial \xi}\right] = -\beta^2\varepsilon^2\left[\frac{1}{h}\frac{\partial}{\partial \eta}\left(\frac{1}{h^2}\frac{\partial hu}{\partial \xi}\right) - \frac{1}{h}\frac{\partial}{\partial \eta}\left(\frac{1}{h^2}\frac{\partial hv}{\partial \eta}\right)\right] - \varepsilon\frac{1}{h}\frac{\partial p}{\partial \xi} - 2\gamma\varepsilon u + \gamma^2\varepsilon\frac{\partial h}{\partial \xi} \tag{3}$$

and

$$\frac{\partial hv}{\partial \xi} + \frac{\partial hu}{\partial \eta} = 0 \tag{4}$$

where $\vec{u} = u\vec{e}_\eta + v\vec{e}_\xi$ and the dimensionless scale factor $h = (\sinh^2\xi + \sin^2\eta)^{\frac{1}{2}}$. The last terms of the momentum equations are respectively the coriolis and centrifugal contributions of the rotating reference frame. In the latter, the radial position vector has been expressed as $\vec{r} = \vec{e}_\xi h\partial/\partial\xi - \vec{e}_\eta \partial h/\partial\eta$. On the surface of the cylinder, taken to be the coordinate surface $\xi = \xi_0$, $u = v = 0$. As $\xi \to \infty$ and for $t = 0$, the solution must match with that representing a time dependent inviscid flow.

We shall assume that the outer dependent variables (lower case) have expansions of the form

$$\begin{aligned} u(\xi,\eta,t;\varepsilon) &\sim u_0(\xi,\eta) + \varepsilon u_1(\xi,\eta,t) + \varepsilon^2 u_2(\xi,\eta,t) + \cdots \\ v &\sim v_0 + \varepsilon v_1 + \varepsilon^2 v_2 + \cdots \\ p &\sim p_0 + \varepsilon p_1 + \varepsilon^2 p_2 + \cdots \\ \psi &\sim \psi_0 + \varepsilon\psi_1 + \varepsilon^2\psi_2 + \cdots \end{aligned} \tag{5}$$

as $\xi \to 0$, where the streamfunction satisfying Eq. (4) is given by $u = h^{-1}\partial\psi/\partial\xi$ and $v = -h^{-1}\partial\psi/\partial\eta$.

The outer flow, being initially irrotational except for a constant background vorticity of magnitude 2γ associated with the rotating frame, remains strictly irrotational in subsequent approximations. Hence, the outer fluid motion is described spatially by

$$\nabla^2\psi_0 = 2 \tag{6}$$

and

$$\nabla^2\psi_n = 0 \quad \text{for } n > 0 \tag{7}$$

together with appropriate boundary conditions. At $t = 0$, $\psi_n = 0$ for $n > 0$. The Bernoulli forms of Eqs. (2) and (3),

$$\frac{\partial u}{\partial t} = -\frac{\varepsilon}{h}\frac{\partial}{\partial \eta}\left(p + \frac{u^2+v^2}{2}\right) - \varepsilon\gamma^2\frac{\partial h}{\partial \eta} \tag{8}$$

$$\frac{\partial v}{\partial t} = -\frac{\varepsilon}{h}\frac{\partial}{\partial \xi}\left(p + \frac{u^2+v^2}{2}\right) + \varepsilon\gamma^2\frac{\partial h}{\partial \xi} \tag{9}$$

serve to determine the pressure distribution.

The streamfunction satisfying (6) and describing the initial inviscid flow about the elliptic cylinder is

$$\tilde{\psi} = -(1-\gamma)e^{\xi_0}\sinh(\xi-\xi_0)\sin(\eta-\alpha_0-\gamma\varepsilon t) + \frac{\gamma}{4}\left[\cosh 2\xi - \cosh 2\xi_0 - \cos 2\eta\left(e^{-2(\xi-\xi_0)} - 1\right)\right].$$

It is normalized to zero on $\xi = \xi_0$ and, at a distance, in the original (dimensional) variables, approaches

$$-U_s\left(r - \frac{r_0^2}{r}\right)\sin(\eta-\alpha_0-\Omega t) + \frac{\Omega}{2}\left(r^2 - r_0^2\right)$$

(let $r = Le^{\xi}/2$ and $\xi \to \infty$ while $L \to 0$ such that r is fixed) which is recognized as the solution for the corresponding flow about a circular cylinder of radius r_0. Expanding $\tilde{\psi}$ for small ε we get

$$\begin{aligned} \tilde{\psi} &= \tilde{\psi}_0 + \varepsilon\tilde{\psi}_1 + \varepsilon\tilde{\psi}_2 + \cdots \\ &= -(1-\gamma)e^{\xi_0}\sinh(\xi-\xi_0)\sin(\eta-\alpha_0) \\ &\quad + \frac{\gamma}{4}\left[\cosh 2\xi - \cosh 2\xi_0 - \cos 2\eta\left(e^{-2(\xi-\xi_0)} - 1\right)\right] \\ &\quad + \varepsilon\gamma(1-\gamma)te^{\xi_0}\sinh(\xi-\xi_0)\cos(\eta-\alpha_0) \\ &\quad + \varepsilon^2\frac{\gamma^2}{2}(1-\gamma)t^2e^{\xi_0}\sinh(\xi-\xi_0)\sin(\eta-\alpha_0) + \cdots \end{aligned} \tag{10}$$

For the inner expansions, the coordinate normal to the surface is rescaled in accordance with the expectation that a length scale different than the geometric length L is more appropriate for characterizing local variations. This is accomplished by

applying a stretching transformation to the coordinate ξ; the required stretch being that which is sufficient to restore a viscous presence in the limit $\epsilon \to 0$ (cf. equ. (2)). Define the stretched variable $\bar{\xi}$ by

$$\xi - \xi_o = \epsilon\, \bar{\xi} \tag{11}$$

and assume that the inner dependent variables (upper case), as functions of $\bar{\xi}$, have expansions of the form

$$\begin{aligned} u(\xi,\eta,t;\epsilon) &\sim U_o(\bar{\xi},\eta,t) + \epsilon U_1(\bar{\xi},\eta,t) + \dots \\ v &\sim \epsilon\{V_o + \epsilon V_1 + \dots\} \\ p &\sim P_o + \epsilon P_1 + \dots \\ \psi &\sim \epsilon\{\Psi_o + \epsilon \Psi + \dots\} \end{aligned} \tag{12}$$

as $\epsilon \to 0$. Further, express the scale factor as a function of $\bar{\xi}$ by expanding h in a Taylor series for small ϵ.

$$\begin{aligned} h(\xi,\eta) &= h(\xi_o,\eta) + \epsilon\bar{\xi}\left(\frac{\partial h}{\partial \xi}\right)_{\xi_o} + \cdots \\ &\equiv h_o(\eta)\left[1 + \epsilon\bar{\xi}\, h_1(\eta) + \cdots\right] \end{aligned}$$

Upon substituting the expansions for u, v, and p (Eq. 12) into the governing equations (2) and (3) and equating like powers of ϵ, we get, for the first inner approximation,

$$\frac{\partial U_o}{\partial t} - \frac{\beta^2}{h_o^2}\frac{\partial^2 U_o}{\partial \bar{\xi}^2} = 0 \tag{13}$$

$$\frac{\partial P_o}{\partial \bar{\xi}} = 0 \tag{14}$$

and, for the second approximation,

$$\begin{aligned} \frac{\partial U_1}{\partial t} - \frac{\beta^2}{h_o^2}\frac{\partial^2 U_1}{\partial \bar{\xi}^2} = &-\frac{1}{h_o}\frac{\partial P_o}{\partial \eta} - \left[\frac{U_o}{h_o}\frac{\partial U_o}{\partial \eta} + \frac{V_o}{h_o}\frac{\partial U_o}{\partial \bar{\xi}}\right] \\ &- 2\frac{\beta^2}{h_o^2} h_1 \bar{\xi}\frac{\partial^2 U_o}{\partial \bar{\xi}^2} - \gamma^2\frac{\partial h_o}{\partial \eta} \end{aligned} \tag{15}$$

$$\begin{aligned} -\frac{1}{h_o}\frac{\partial P_1}{\partial \bar{\xi}} = &\frac{\partial V_o}{\partial t} - \frac{U_o^2}{h_o} h_1 + \beta^2\frac{1}{h_o}\frac{\partial}{\partial \eta}\left(\frac{1}{h_o}\frac{\partial U_o}{\partial \bar{\xi}}\right) \\ &+ 2\gamma U_o - \gamma^2 h_o h_1 \end{aligned} \tag{16}$$

Boundary and initial conditions on U_o and U_1 are

$U_o = 0$ at $\bar{\xi} = 0$, $t > 0$ (17)

U_o matches outer solution as $\bar{\xi} \to \infty$, $t > 0$

and for $t = 0$, $\bar{\xi} > 0$

and $U_1 = 0$ at $\bar{\xi} = 0$ and $t = 0$ (18)

U_1 matches outer solution as $\bar{\xi} \to \infty$

The streamfunction (zero on surface) is determined by integrating the tangential velocity component in the direction normal to the surface:

$$\begin{aligned} \Psi &= \int_{\xi_o}^{\xi} u\, h\, d\xi \\ &\sim \epsilon\left\{ h_o \int_0^{\bar{\xi}} U_o\, d\bar{\xi} + \epsilon h_o \int_0^{\bar{\xi}} (U_1 + \bar{\xi} h_1 U_o)\, d\bar{\xi} \right. \\ &\qquad \left. + \cdots \right\} \end{aligned} \tag{19}$$

IV. The Solution for $R^{-1} = O(\epsilon)$

The method of solution is formally the same as that of Wang. We shall, therefore, merely present a sketch of the procedural details. Equations for the inner tangential velocity and outer streamfunction perturbations are alternately solved. Where lacking, boundary conditions and, in the case of the inner solution, tangential pressure variation are supplied through matching conditions. For this, van Dyke's asymptotic matching principle is adequate.[7] Step-by-step we may also check and confirm our choice of an asymptotic sequence.

The zero-th order outer solution is (cf. equ. (10))

$$\psi_o = \bar{\psi}_o \tag{20}$$

and the corresponding velocity components are

$$\begin{aligned} u_o = \frac{1}{h}\left\{ -(1-\gamma)\, e^{\xi_o}\cosh(\xi-\xi_o)\sin(\eta-\alpha_o) \right. \\ \left. + \frac{\gamma}{2}\left[\sinh 2\xi + \cos 2\eta\, e^{-2(\xi-\xi_o)}\right]\right\} \end{aligned} \tag{21}$$

and

$$\begin{aligned} v_o = -\frac{1}{h}\left\{ -(1-\gamma)\, e^{\xi_o}\sinh(\xi-\xi_o)\cos(\eta-\alpha_o) \right. \\ \left. + \frac{\gamma}{2}\sin 2\eta\left(e^{-2(\xi-\xi_o)} - 1\right)\right\} \end{aligned} \tag{22}$$

The solution of Eq. (13) for the zeroth order of the inner expansion is

$$U_o = u_o(\xi_o,\eta)\, \mathrm{erf}\,\zeta \quad , \quad \zeta = \frac{h_o\bar{\xi}}{2\beta\sqrt{t}} \tag{23}$$

where the factor $u_0(\xi_0,\eta)$ has been identified by matching inner and outer tangential velocity components. U_0 is, of course, Rayleigh's solution. The streamfunction in this approximation is obtained from Eq. (19).

$$\Psi_o = 2\beta t^{1/2} u_o(\xi_o,\eta)\left[\zeta\,\mathrm{erf}\,\zeta + \frac{1}{\sqrt{\pi}}\left(e^{-\zeta^2} - 1\right)\right] \tag{24}$$

The surface boundary condition for ψ_1 is found from matching the inner and outer streamfunction expansions, (12) and (5), with ψ_0 and Ψ_0 given by Eqs. (20) and (24). This yields the matching condition

$$\Psi_1(\xi_o,\eta,t) = -\frac{2\beta t^{1/2}}{\sqrt{\pi}}\, u_o(\xi_o,\eta) \tag{25}$$

ψ_1 is then obtained as the solution of the Laplace equation with the additional condition that

$$\psi_1 = \bar{\psi}_1 + t^{1/2}\cdot(\text{bounded quantity}) \text{ as } \xi \to \infty.$$

Both the condition on the surface and that at infinity satisfy the spatial-temporal separability requirement and vanish at $t = 0$. Since $\bar{\psi}_1 = 0$ for $\xi = \xi_0$, the solution for the first order perturbation to the outer streamfunction can be written as

$$\psi_1 = \bar{\psi}_1 + \hat{\psi}_1 \tag{26}$$

with $\hat{\psi}_1$ satisfying (25) and expressed as a Fourier series,

$$\hat{\Psi}_1 = -\frac{2\beta t^{1/2}}{\sqrt{\pi}}\left[\frac{A_0}{2} + \sum_{k=1}^{\infty}\left(A_k\cos k\eta + B_k\sin k\eta\right)e^{-k(\xi-\xi_o)}\right] \tag{27}$$

whose coefficients may be evaluated recursively from the complete elliptic integrals of the first and second kind with the parameter depending on the eccentricity of the elliptic cylinder. Convergence of the series is quite rapid for fatter shapes but, as expected, much slower for eccentricities approaching unity.

The fluid surface upon which the inviscid streamfunction vanishes to first order no longer coincides with the surface of the cylinder. It has been displaced by the growing boundary layer as if the body were deforming in time and presenting a larger obstacle to the inviscid fluid motion. We will return to this later in connection with the pressure distribution.

The first order perturbation, U_1, to the inner tangential component of velocity is the solution of equ. (15), an inhomogeneous diffusion equation, with the accompanying initial and boundary conditions. Recall equ. (14) that, in the first approximation, the pressure was constant across the boundary layer. Hence, an expression for $\partial P_0/\partial\eta$ is found by matching with the outer expansion for this derivative of pressure. From equ. (8), this gives

$$\frac{\partial P_0}{\partial \eta} = \left(\frac{\partial p_0}{\partial \eta}\right)_{\xi_0} = -h_0\left[\frac{\partial u_1}{\partial t} + \frac{1}{h_0}\frac{\partial}{\partial \eta}\left(\frac{u_0^2+v_0^2}{2}\right) + \gamma^2\frac{\partial h}{\partial \eta}\right]_{\xi_0} \tag{28}$$

With this and other substitutions, the equation for U_1 becomes

$$\frac{\partial U_1}{\partial t} - \frac{\beta^2}{h_0}\frac{\partial^2 U_1}{\partial \xi^2} = \left[\frac{u_0 u_0'}{h_0}E(\xi) + g(\eta)\right] + t^{-\frac{1}{2}}\left[u_0 f(\eta)\xi^2 e^{-\xi^2} + F(\eta)\right] \tag{29}$$

where

$$E(\xi) = 1 - \operatorname{erf}\xi + \frac{2}{\sqrt{\pi}}\xi e^{-\xi^2}\operatorname{erf}\xi + \frac{2}{\pi}e^{-\xi^2}\left(e^{-\xi^2}-1\right)$$

$$g(\eta) + t^{-\frac{1}{2}}F(\eta) = \left(\frac{\partial u_1}{\partial t}\right)_{\xi_0} = \left[\frac{\partial}{\partial t}\left(\frac{1}{h}\frac{\partial \tilde{\psi}_1}{\partial \xi} + \frac{1}{h}\frac{\partial \hat{\psi}_1}{\partial \xi}\right)\right]_{\xi_0}$$

$$f(\eta) = \frac{q = h_1}{\sqrt{2}\,h_0}$$

and

$$u_0 = u_0(\xi_0,\eta)\ ,\quad u_0' = du_0(\xi_0,\eta)/d\eta$$

The solution prescribed by the inhomogeneity has the form

$$U_1 = t\,y(\xi,\eta) + t^{\frac{1}{2}}z(\xi,\eta) \tag{30}$$

When the boundary conditions $y(0,\eta) = z(0,\eta)$ are applied, there still remains an unknown function of η in each of the solutions y and z which is determined from matching with the outer expansion for the tangential velocity component. The results are

$$y = -\frac{u_0 u_0'}{h_0}\left\{\frac{2}{3\pi}(1+2\xi^2) - \frac{1}{2}(1-2\xi^2)\operatorname{erf}\xi - \frac{3}{\sqrt{\pi}}\xi e^{-\xi^2}\operatorname{erf}\xi - \frac{2}{\pi}e^{-\xi^2}\left(e^{-\xi^2}-\frac{3}{2}\right) - 2\xi^2 - \left(\frac{2}{3\pi}+\frac{1}{2}\right)\left[(1+2\xi^2)\operatorname{erf}\xi + \frac{2\xi}{\sqrt{\pi}}e^{-\xi^2}\right]\right\} + g\left[(1+2\xi^2)\operatorname{erf}\xi + \frac{2}{\sqrt{\pi}}\xi e^{-\xi^2} - 2\xi^2\right]$$

and

$$z = \left[\frac{2\beta}{h_0}\left(\frac{\partial u_0}{\partial \xi}\right)_{\xi_0} + 2\sqrt{\pi}F + u_0 f\frac{\sqrt{\pi}}{4}\right]\xi - 2\sqrt{\pi}F\left[\xi\operatorname{erf}\xi + \frac{1}{\sqrt{\pi}}\left(e^{-\xi^2}-1\right)\right] - u_0 f\left[\frac{\sqrt{\pi}}{4}\xi\operatorname{erf}\xi - \frac{1}{2}\xi^2 e^{-\xi^2}\right]$$

Performing the integrations indicated in equ. (19), we obtain

$$\Psi_1 = t\,G(\xi,\eta) + t^{3/2}H(\xi,\eta) \tag{31}$$

with

$$G = 4\beta^2\frac{h_1}{h_0}u_0\left[\frac{1}{4}(2\xi^2-1)\operatorname{erf}\xi + \frac{\xi}{2\sqrt{\pi}}e^{-\xi^2}\right] + 2\beta\left\{\left[\frac{2\beta}{h_0}\left(\frac{\partial u_0}{\partial \xi}\right)_{\xi_0} + 2\sqrt{\pi}F + u_0 f\frac{\sqrt{\pi}}{4}\right]\frac{\xi^2}{2} - 2\sqrt{\pi}F\left[\frac{1}{4}(1+2\xi^2)\operatorname{erf}\xi + \frac{\xi}{\sqrt{\pi}}\left(\frac{1}{2}e^{-\xi^2}-1\right)\right] - u_0 f\frac{\sqrt{\pi}}{4}\left[\frac{1}{4}(2\xi^2-3)\operatorname{erf}\xi + \frac{3}{2\sqrt{\pi}}\xi e^{-\xi^2}\right]\right\}$$

and

$$H = 2\beta\left\{-\frac{u_0 u_0'}{h_0}\left[\frac{2}{3\pi}\left(\xi+\frac{3}{2}\xi^3\right) + \frac{1}{2}\left(\xi-\frac{3}{2}\xi^3\right)\operatorname{erf}^2\xi + \frac{1}{6\sqrt{\pi}}(11-4\xi^2)e^{-\xi^2}\operatorname{erf}\xi - \frac{8}{3\sqrt{3\pi}}\operatorname{erf}(\sqrt{2}\xi) + \frac{2}{3\sqrt{\pi}}\operatorname{erf}\xi - \frac{1}{3\pi}\xi e^{-2\xi^2}\right] + \left[\frac{u_0 u_0'}{h_0}\left(\frac{2}{3\pi}+\frac{1}{2}\right) + g\right]\cdot\left[\left(\xi+\frac{2}{3}\xi^3\right)\operatorname{erf}\xi + \frac{2}{3\sqrt{\pi}}\left(\xi^2+1\right)e^{-\xi^2} - \frac{2}{3\sqrt{\pi}}\right] - \left(\frac{u_0 u_0'}{h_0} + g\right)\frac{2}{3}\xi^3\right\}.$$

The surface condition for the second order perturbation to the outer streamfunction is easily obtained, again by matching, but the solution is complicated by the presence of the function $F(\eta)$, itself expressed as a series. The trend is to increasingly more cumbersome perturbations, equations, and solutions. We, therefore, have terminated the development at this stage, though it turns out to have been perhaps an unfortunate decision. Since there are terms of the inner solution having no ε^2-match (their match being precisely the surface condition on ψ_2), in the composite expansion, the inner solution will have a nonexponentially decaying influence at large distances from the body. Nevertheless, this influence is of $O(\varepsilon^2)$

A uniformly valid composite expansion is obtained by adding the inner and outer streamfunction expansions and deleting the matching conditions, which occur twice in the sum. Thus,

$$\psi_c = \psi_0 + \varepsilon(\hat{\psi}_1 + \hat{\psi}_1) + \varepsilon(\psi_0 + \varepsilon\psi_1) - \psi^* \tag{32}$$

in which

$$\psi^* = h_0(\xi-\xi_0)u_0 - \frac{\varepsilon}{\sqrt{\pi}}2\beta t^{\frac{1}{2}}u_0 + (\xi-\xi_0)^2\frac{1}{2}\left(\frac{\partial^2\tilde{\psi}_0}{\partial\xi^2}\right)_{\xi_0} + \varepsilon(\xi-\xi_0)h_0 u_1(\xi_0,\eta)$$

consists of a set of the matching conditions and ψ_c is expressed uniformly in the outer variable ξ.

Instantaneous vorticity contours, where the vorticity is given by $\nabla^2\psi_c$, are overlaid on the instantaneous streamlines in Figs. 2-5 for an ellipse of eccentricity 2/3, a Reynolds number of approximately 1000, a 15° initial angle of attack, and at a dimensionless time $U_\infty t/L = 0.6$. $\gamma = 0.4$ for the rotating ellipse--a quite high pitch rate $\Omega L/U_\infty = 2/3$)--which gives an instantaneous angle of attack of $\sim 28.7°$ at time 0.6. The circled numbers in these drawings show the approximate location of local surface vorticity extrema.

We have found that, since the time domain of validity shrinks as the local curvature is increased, the only appreciable effect of increasing the eccentricity is to reduce the size of the flow features; when drawn scaled to the same tip radius, the patterns are essentially identical. Further, as time advances, flow structures merely continue to grow. For example, the trailing edge vortex shows no inclination to depart and, in trials with a non-rotating circular cylinder, no secondary recirculating flow structures formed. Obviously convective influences are not strongly represented in a diffusion dominated solution. For this particular ellipse and Reynolds number, improbable distortion in the flow field appeared for times greater than 1.0 or 1.2. Direct comparison with experiment might only be feasible for considerably smaller times.

Streamlines and vorticity contours for the rotating cylinder (Figs. 4,5) are depicted relative to the body fixed frame. This casts a slight shadow on the interpretation of streamline patterns. However, the interpretation of flow structures, such as a separation bubble, remain fairly reliable, especially when observed in a continuum of rotation rates, although the particular form may vary. This indicates a need to incorporate all available descriptions, including the pressure and vorticity fields, into interpretations. Transformation from the body frame to one that is instantaneously coincident but non-rotating,

$$\psi_{nr} = \psi_b - \frac{\gamma}{2}(\cosh^2\xi - \sin^2\eta) ,$$

accomplishes little in the way of aiding the interpretation of streamlines but it shows that the pattern of vorticity contours is invariant, the values only differing by 2γ. (In the transformed system, the surface of the rotating cylinder is no longer a streamline; streamlines depart from that portion of the surface which is advancing into the fluid and are drawn to that portion which is retreating.)

We make the following observations:

1. Without rotation (Fig. 3), the streamline pattern is a deformation of the early symmetric pattern of oscillating flow behind a circular cylinder. At the instant depicted, the saddle point has been pulled apart such that the trailing edge vortex is no longer bounded by a closed stagnation streamline (a piecewise continuous streamline in the fluid whose terminal points are body stagnation points); the vortex is free to depart into the wake. Such is concomitant to the establishment of the Kutta condition at the trailing edge. In contrast to this, for the rotating body (Fig. 5), the trailing edge vortex is confined by a closed stagnation streamline (as if the saddle point were pulled apart across the other two vertices) and more closely resembles a separation bubble. Thus, the establishment of the Kutta condition is temporarily, at least, suspended.

2. In the neighborhood of the leading edge (Figs. 2,4), we note the presence of very high values of surface vorticity for the case of fixed angle of attack as compared to those on the rotating ellipse. This is one indication of the fairly sharp turn the flow must make about the leading edge from the stagnation point and supports the view that the apparent angle of attack is reduced (indeed eliminated in the case drawn) by rotation. Additional support comes from the presence of the cell of positive vorticity lying just off the leading edge which is completely absent in the case of rotation. Its presence may be taken as a precursor or sign of an incipient leading edge separation bubble and conversely for its absence. (A separation bubble is not evident from the streamline pattern for such a low angle of attack. At $\sim 28°$, the instantaneous angle of attack of the rotating body, a bubble is well developed.)

V. Pressure Distribution and Lift

The zeroth order surface pressure distribution is first that of the outer inviscid flow impressed across the bl ($P_o(\eta) = p_o(\xi_o,\eta)$, ct. Eq. (14)). Integrating Eqs. (8,9) along a path running from a point at infinity to an arbitrary point (ξ_o,η) on the surface of the ellipse and expressing the result as a pressure coefficient, we get (for $\gamma \neq 1$, i.e., $U_\infty \neq 0$)

$$C_{p_o} = \frac{p_o - p_{o_\infty}}{\frac{1}{2}(1-\gamma)^2} = 1 - \frac{2}{(1-\gamma)^2}\left\{ -\frac{\gamma^2}{2}\left(\sinh^2\xi_o - \sin^2\eta\right) + \left[\frac{1}{2}\left(u_o^2 + v_o^2\right) + \frac{\partial\phi_1}{\partial t}\right]_{\xi_o,\eta}\right\} \tag{33}$$

where ϕ_1 is a velocity potential defined by $\vec{u}_1 = \nabla\phi_1$ for the time dependent first order (outer) velocity,

$$\phi_1 = t\,\gamma(1-\gamma)\,e^{\xi_o}\cosh(\xi-\xi_o)\sin(\eta-\alpha_o) + \frac{2\beta t^{\frac{1}{2}}}{\sqrt{\pi}}\sum_{k=1}^{\infty}\left(A_k\sin k\eta - B_k\cos k\eta\right)e^{-k(\xi-\xi_o)}$$

in which the first term stems from the changing angle of incidence of the distant stream and the second represents the displacement affect of the growing bl. The pressure singularity at $t = 0$ is traceable to the impulsive onset of motion: The initial rate of growth of the BL, estimated by the initial pseed at which vorticity penetrates into the fluid with penetration depth taken in the usual sense as that depth at which the vorticity has a value 1/e times its surface value, is singular at $t = 0$, so also is the outer inviscid flow response.

In order to determine the first order pressure perturbation, inner or outer, it would be necessary to know the second order perturbation to the outer streamfunction, ψ_2, or at least $\partial\psi_2/\partial\xi$ calculated at ξ_o. This should not be too difficult to calculate but has not been included here.

Lift is determined from the integral

$$C_l = -\cosh\xi_o\cos\alpha(t)\int_0^\pi\left[C_p(\eta) - C_p(2\pi-\eta)\right]\sin\eta\,d\eta \tag{34}$$

in which $\alpha(t)$ is the instantaneous angle of attack and the projection of surface area onto the chord is given by the ratio of $|dx(\eta)| = \cosh\zeta_0 \sin\eta d\eta$ to $hd\eta$. This is easily integrated to give

$$C_L = \cos\alpha(t)\left[\frac{2\gamma}{(1-\gamma)}\pi\cos\alpha_0 + \frac{2}{(1-\gamma)^{\frac{1}{2}}}\sqrt{\pi}\,\beta\,t^{-\frac{1}{2}}A_1\cosh\xi_0\right] \quad (35)$$

with

$$A_1 = \frac{1}{\pi}\int_{-\pi}^{\pi} u_0(\xi_0,\eta)\cos\eta\,d\eta$$

the only remaining Fourier coefficient.

The pressure (C_p) distributions for the rotating and non-rotating cylinders are drawn for comparison in Fig. 6 and the associated values of lift for various times are presented in Table 1. For the rotating cylinder, we notice the extended region of favorable pressure gradient on the upper surface which qualitatively resembles the distribution on a nonrotating elliptic cylinder at a very small or zero angle of attack. The pressure drop near the trailing edge, also on the upper surface, occurs under the influence of the trailing edge vortex. In contrast, the non-rotating body exhibits the usual extended region of adverse gradient and diagonal symmetry. Lift is seen to be substantially higher for the rotating ellipse than for that at a fixed angle of attack. The $t^{-1}/2$ decay is, in this approximation, the vestige of the impulsive start.

The dimensionless circulation inferred from the presence of lift is $C_L/(1-\gamma)$. At the time of this writing, we have not succeeded in spatially integrating the vorticity to confirm the values of circulation. In part, the difficulty lies in the non-exponential decay of vorticity mentioned previously.

VI. Conclusion

Within the limitations of the solution, we have seen here the addition of pitching motion or rotation suppresses the early formation of leading edge separation bubbles by creating a situation in which the effective angle of attack is much reduced. We have also found the initial lift to be enhanced and the establishment of the Kutta condition at the trailing edge to have been put in abeyance by rotation.

Acknowledgment

This work was supported by the Air Force Office of Scientific Research under Grant AFOSR-~~80-0097~~ 81-0097.

References

[1] Nash, J.F. and Scruggs, R.M., "Unsteady Boundary Layers with Reversal and Separation," AGARD Paper No. 18, Symposium on Unsteady Aerodynamics, Ottawa, CA, September 1977.

[2] Sear, W.R. and Telionis, D.P., "Boundary-layer Separation in Unsteady Flow," SIAM Journal of Applied Mathematics, Vol. 28, 1975, pp. 215-235.

[3] Goldstein, S. and Rosenhead, L., "Boundary Layer Growth," Proceedings of the Cambridge Philosophical Society, Vol. 32, 1936, pp. 392-401.

[4] Stuart, J. T., "Unsteady Boundary Layers," Laminar Boundary Layers, L. Rosenhead, ed., Oxford University Press, London, 1963, Chapter VII.7.

[5] Batchelor, G.K., An Introduction to Fluid Dynamics, Cambridge University Press, Cambridge, 1967, Chapter 5, (pp. 314-331).

[6] Wang, C.-Y., "Separation and Stall of an Impulsively Started Elliptic Cylinder," Journal of Applied Mechanics, Vol. 34, 1967, pp. 823-828.

[7] VanDyke, M., Perturbation Methods in Fluid Mechanics, Academic Press, New York, 1964, 5.7, pp. 87-90.

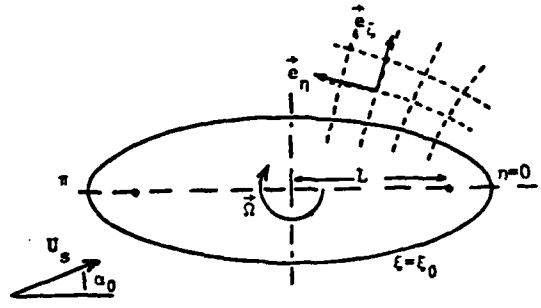

Fig. 1. Physical configuration.

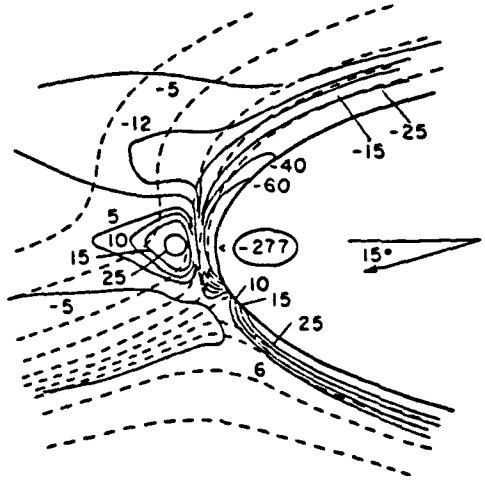

Fig. 2. Leading edge of elliptic cylinder, translation to left at 15° angle of attack at time $U_c t/L = 0.6$. Streamlines (dashed) and vorticity contours (solid, labeled) are overlaid. Circled values indicate approximate location of vorticity extrema.

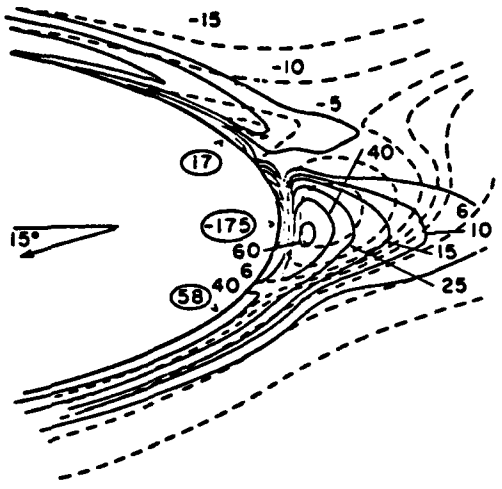

Fig. 3. Trailing edge of elliptic cylinder translating at 15° angle of attack at time 0.6 (cf. Fig. 2).

	t = .2	.4	.6	.8	1.0
γ = 0.0	.180	.127	.104	.090	.080
0.4	4.104	3.891	3.704	3.510	3.301

Table 1. Calculated lift versus time

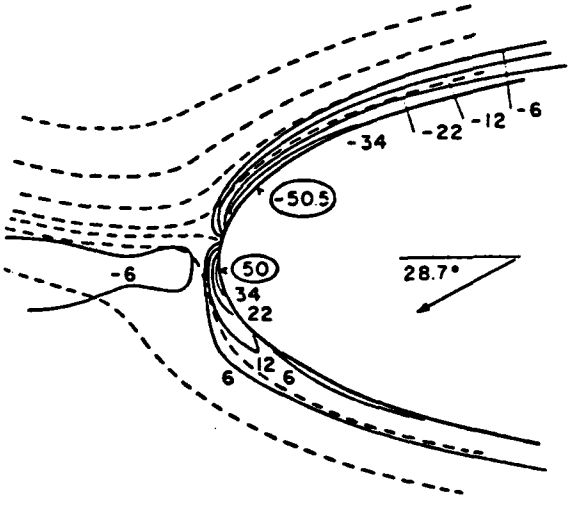

Fig. 4. Leading edge of elliptic cylinder rotating clockwise and translating at an instantaneous angle of attack 28.7°, time 0.6, and rotation rate $\Omega L/U_c$ = 2/3. (cf. Fig. 2)

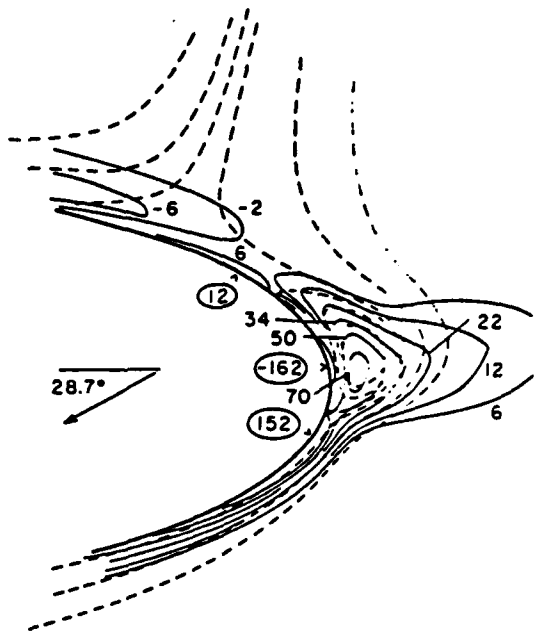

Fig. 5. Trailing edge of elliptic cylinder rotating and translating at an instantaneous angle of attack of 28.7° (pitch-up from 15°), for time 0.6 and rotation rate 2/3 (cf. Fig. 2).

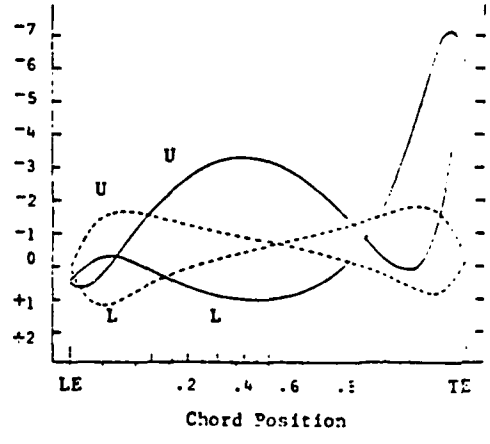

Fig. 6. C_p distribution on elliptic cylinders: Dashed curve is for cylinder translating at 15° angle of attack: solid curve is for cylinder translating and rotating (pitch-up) from an initial angle of attack of 15°. Time 0.2. Upper and lower surfaces are denoted by U and L.